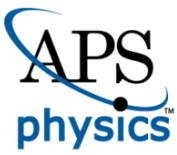

Solvation-Driven Electrochemical Actuation

Alain Boldini, Youngsu Cha, and Maurizio Porfiri

Phys. Rev. Lett. **126**, 046001 — Published 27 January 2021

DOI: 10.1103/PhysRevLett.126.046001

Solvation-driven electrochemical actuation

Alain Boldini
Department of Mechanical and Aerospace Engineering, New York University Tandon School of Engineering, Brooklyn, New York 11201, USA

Youngsu Cha
Center for Intelligent & Interactive Robotics, Korea Institute of Science and Technology, Seoul, 02792, Republic of Korea

Maurizio Porfiri*
Department of Mechanical and Aerospace Engineering and Department of Biomedical Engineering, New York University Tandon School of Engineering, Brooklyn, New York 11201, USA

(Dated: December 23, 2020)

We demonstrate a novel principle of contactless actuation for ionic membranes in salt solution based on solvation. Actuation is driven by differential swelling of the sides of the membrane, due to co-migrating water in the solvation shells of mobile ions. We validate our theory through a series of experiments, which unravel a strong dependence of membrane deflection on the hydration numbers of mobile ions in the external solution and membrane. Our study suggests a critical role of solvation in the chemoelectromechanics of natural and artificial selectively-permeable membranes.

Introduction.–Solvation – the interaction between solute and solvent molecules – is a widely studied phenomenon in physical chemistry [1, 2]. Since the seminal studies of Lewis [3], Kielland [4], and Born [5], our understanding of this phenomenon has greatly benefited from computational analyses across physical scales [6–8] and experimental assays [9, 10].

In water-based electrolyte solutions, water molecules interact with dissolved monoatomic ions through hydrogen and dipole-dipole interactions, forming solvation shells around them [11]. Hydration numbers quantify "the time-average numbers of water molecules residing in the first hydration shells of ions (and in the second, if formed)" [12]. In solution, larger ions have larger hydration numbers, since more water molecules can fit in the hydration shells, but the strength of the bonds is smaller due to the lower charge density [2]. Thus, diffusivities of small univalent cations can be lower than larger cations, in contrast with Stokes-Nernst-Einstein's predictions [12].

Beyond ion diffusivity, solvation plays a critical role in a wide realm of physical and electrochemical properties of electrolyte solutions [13], from mass density [14] to surface tension [15] and color [16]. Biological systems are also greatly affected by solvation, which contributes to molecular assembly, conformation, and, ultimately, functionality of macromolecules, such as proteins and nucleic acids [17, 18]. To date, no empirical evidence has been gathered on the effect of solvation on the mechanical response of macroscopic systems.

Here, we demonstrate solvation-driven actuation of ionic membranes in salt solution under an external electric field. We draw inspiration from experimental observations of contactless actuation of polyelectrolyte gels [19, 20] and ionic membranes [21, 22]. Through theoretical insight and empirical findings, we examine this new physical phenomenon.

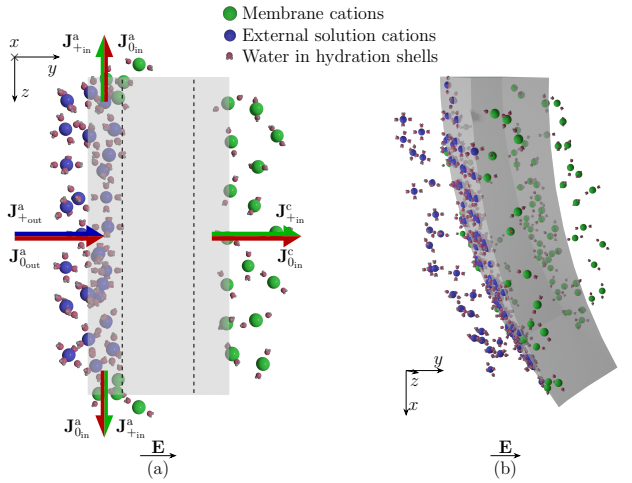

FIG. 1. Physics of solvation-driven actuators. (a) Top view of the undeformed membrane, whose anode (left) and cathode (right) are delimited by dashed lines. Cations in the external solution enter the membrane at the anode ($\mathbf{J}^{a}_{+_{out}}$) and force cations initially in the membrane to diffuse in the external solution from the sides ($\mathbf{J}^{a}_{+_{in}}$). Other membrane cations leave the membrane at the cathode ($\mathbf{J}^{c}_{+_{in}}$). Solvated cations bring along water molecules in their solvation shells ($\mathbf{J}^{a}_{0_{out}}$, $\mathbf{J}^{a}_{0_{in}}$, and $\mathbf{J}^{c}_{0_{in}}$). (b) Migration of solvated cations causes macroscopic actuation due to localized volume changes at the membrane anode (swelling) and cathode (contraction). **E** indicates the direction of the electric field.

Theory.–To illustrate the principles of solvation-driven actuation, we focus on cation-exchange membranes, where negative coions are fixed to the polymer backbone

and positive counterions move in the hydrating solution [23]. Under an external electric field, cations and anions in the external solution are forced to migrate. Due to membrane coions, anions in the external solution are selectively prevented from entering the membrane, while cations can enter and leave the membrane. The motion of these cations causes concentration changes within the nanometer-thick double layers at the interface with the external solution [24], which identify the membrane anode and cathode. Specifically, cations in the external solution enter the anode, forcing out cations initially inside the membrane from the sides of the anode (Fig. 1). Concurrently, membrane cations leave the cathode and diffuse in the external solution due to the electric field. Water molecules in solvation shells move with the corresponding solvated cations [12, 25] [26], eliciting localized swelling and contraction at the anode and cathode of the membrane, respectively. This differential volumetric deformation causes macroscopic bending.

As a first approximation, we model the membrane as a cantilever Euler-Bernoulli beam of length l and thickness $2H$. We use a right-handed coordinate system with $x-$ and y-axis running along the beam axis and thickness, see Fig. 1. We consider a stress-free reference configuration for the membrane, with uniform concentrations C_0^{ref} of water and C_+^{ref} of cations that form the hydrating solution. Following standard practice in mixture theories [27], we exploit incompressibility of the solution and dry membrane [28] to relate the local volume of the mixture to changes in the concentrations of water and cations, driven by the diffusion of cations at the membrane-solution interfaces. We hypothesize that the corresponding volumetric deformation is isotropic, generating a spherical pre-strain

$$\boldsymbol{\varepsilon}^{\mathrm{C}} = \frac{1}{3}\left(\mathcal{V}_0\Delta C_0 + \mathcal{V}_+\Delta C_+\right)\boldsymbol{I}. \tag{1}$$

Here, $\mathcal{V}_0$ and $\mathcal{V}_+$ are the molar volumes of water and cations, ΔC_0 and ΔC_+ are the concentration changes of water and cations per unit reference mixture volume, and $\boldsymbol{I}$ is the identity tensor. Finally, we write the axial mechanical strain as $\varepsilon_{xx}^{\mathrm{mec}} = -ky + \varepsilon_0 - \varepsilon_{xx}^{\mathrm{C}}$, and the corresponding axial stress as $\sigma_{xx} = E\varepsilon_{xx}^{\mathrm{mec}}$, where k, ε_0, and E are the curvature, mid-axis strain, and Young modulus of the membrane, respectively.

According to the proposed model, solvated cations initially inside membrane leave the membrane from both the anode and cathode, while solvated cations in the surrounding solution enter the membrane from the anode only. We assume that variations in water concentration are solely due to the co-migration of water in the solvation shells of cations, which are limited to the membrane anode and cathode. If both these regions have thickness ζ, we define

$$\Delta C_i = \begin{cases} \Delta C_{i_{\mathrm{in}}}^{\mathrm{a}} + \Delta C_{i_{\mathrm{out}}}^{\mathrm{a}} & \text{for } y < -H+\zeta \\ \Delta C_{i_{\mathrm{in}}}^{\mathrm{c}} & \text{for } y > H-\zeta \\ 0 & \text{otherwise} \end{cases}, \tag{2}$$

where $i = 0, +$ for water and cations, subscripts "in" and "out" indicate molecules initially inside and outside the membrane, respectively, and "a" and "c" superscripts mark quantities evaluated at the anode and cathode, respectively.

Solvation relates changes in concentrations of water and cations through $\Delta C_{0_{\mathrm{in}}}^{\mathrm{a}} = h_{\mathrm{in}}\Delta C_{+_{\mathrm{in}}}^{\mathrm{a}}$, $\Delta C_{0_{\mathrm{in}}}^{\mathrm{c}} = h_{\mathrm{in}}\Delta C_{+_{\mathrm{in}}}^{\mathrm{c}}$, and $\Delta C_{0_{\mathrm{out}}}^{\mathrm{a}} = h_{\mathrm{out}}\Delta C_{+_{\mathrm{out}}}^{\mathrm{a}}$. Here, $h_{(\cdot)}$ is the average hydration numbers of cations in the membrane; subscripts "in" and "out" indicate whether the cations were initially in the membrane or in the external solution, respectively. The positive trend between hydration number and cations' size in solution is reversed when cations are in the membrane [29, 30]. We utilize as a proxy for average hydration numbers the hydration effects in an organic solvent computed from molecular dynamics simulations (4.0, 3.6, 3.1, and 2.6 for lithium, sodium, potassium, and cesium, respectively [29] [31]).

Since no external bending moment is applied to the membrane, equilibrium requires that $\int_{-H}^{H}\sigma_{xx}y\,\mathrm{d}y = 0$, which yields the curvature as a function of integrals of $\Delta C_+ y$ at the anode and cathode. Assuming uniform bending moment along the membrane, curvature k and tip displacement d are related by $d = \frac{1}{2}kl^2$.

In principle, ζ could be quantified by the Debye screening length λ [32], however, we consider a more realistic estimate $\zeta \approx 10\lambda$ accounting for steric effects that tend to widen the double layers [33] [34]. Since ζ is small with respect to H, we approximate $\int_{-H}^{-H+\zeta}\Delta C_+^{\mathrm{a}} y\,\mathrm{d}y \approx -10H\lambda\Delta\bar{C}_+^{\mathrm{a}}$ and $\int_{H-\zeta}^{H}\Delta C_+^{\mathrm{c}} y\,\mathrm{d}y \approx 10H\lambda\Delta\bar{C}_+^{\mathrm{c}}$, where quantities with a bar indicate averages over the corresponding region, obtained by integrating the spatially-varying cations' concentrations and dividing the result by the thickness of the double layers. Thus, the tip deflection of the membrane is estimated as

$$d = \frac{5}{2}\left(\frac{l}{H}\right)^2\lambda\big[\mathcal{V}_0(\Delta\bar{C}_{+_{\mathrm{in}}}^{\mathrm{a}} - \Delta\bar{C}_{+_{\mathrm{in}}}^{\mathrm{c}})h_{\mathrm{in}} + \mathcal{V}_0\Delta\bar{C}_{+_{\mathrm{out}}}^{\mathrm{a}}h_{\mathrm{out}} + \mathcal{V}_+(\Delta\bar{C}_{+_{\mathrm{in}}}^{\mathrm{a}} - \Delta\bar{C}_{+_{\mathrm{in}}}^{\mathrm{c}} + \Delta\bar{C}_{+_{\mathrm{out}}}^{\mathrm{a}})\big]. \tag{3}$$

Based on these consideration, we have that $\Delta\bar{C}_{+_{\mathrm{out}}}^{\mathrm{a}} > 0$, $\Delta\bar{C}_{+_{\mathrm{in}}}^{\mathrm{a}} < 0$, and $\Delta\bar{C}_{+_{\mathrm{in}}}^{\mathrm{c}} < 0$, while $\Delta\bar{C}_{+_{\mathrm{in}}}^{\mathrm{a}} - \Delta\bar{C}_{+_{\mathrm{in}}}^{\mathrm{c}}$ may be positive or negative depending on whether more cations initially inside the membrane are lost at the cathode or anode, respectively. The depletion of cations from the membrane is bounded by their initial concentration, which is equal to the concentration C_- of coions per unit reference volume for electroneutrality. For typical ionic membranes, such as Nafion$^{\mathrm{TM}}$, C_- is on the order of $10^3\,\mathrm{mol/m^3}$ [35]. On the other hand, the concentration of

cations entering the membrane anode from the external solution is only limited by steric effects. Electrochemical simulations in ionic membranes provide an upper bound for $\Delta\bar{C}^{\mathrm{a}}_{+_{\mathrm{out}}}$ between C_- and $10\,C_-$ (10^3 - $10^4\,\mathrm{mol/m^3}$) [36]. Given the one order of magnitude difference between the two coefficients of h_{in} and h_{out}, we predict a weaker dependence on cations in the membrane than on cations in the external solution.

When $\Delta\bar{C}^{\mathrm{a}}_{+_{\mathrm{out}}}$ is one order of magnitude more than $\Delta\bar{C}^{\mathrm{a}}_{+_{\mathrm{in}}} - \Delta\bar{C}^{\mathrm{c}}_{+_{\mathrm{in}}}$, we expect that pile-up of cations from the external solution at the anode is the dominant mechanism of actuation. For these conditions, Eq. (3) suggests bending of the membrane in the direction of the electric field. For an increase in the cations' size in the external solution, Eq. (3) predicts a decrease in the tip deflection, since larger cations from the external solution transport less water molecules in the membrane.

The effect of the cations' size in the membrane depends on the sign of $\Delta\bar{C}^{\mathrm{a}}_{+_{\mathrm{in}}} - \Delta\bar{C}^{\mathrm{c}}_{+_{\mathrm{in}}}$. At the anode, small cations in the external solution can pile-up at high concentrations, causing depletion of membrane cations ($\Delta\bar{C}^{\mathrm{a}}_{+_{\mathrm{in}}} - \Delta\bar{C}^{\mathrm{c}}_{+_{\mathrm{in}}} < 0$). In this case, larger cations in the membrane would bring out less water at the swelling anode, producing larger tip deflections, as predicted by Eq. (3). With larger cations in the external solution, charge density at the anode is limited by steric effects, such that we can expect cations' depletion at the cathode ($\Delta\bar{C}^{\mathrm{a}}_{+_{\mathrm{in}}} - \Delta\bar{C}^{\mathrm{c}}_{+_{\mathrm{in}}} > 0$). In this case, Eq. (3) predicts that larger cations in the membrane would beget smaller tip deflections, since less water would migrate out of the membrane from the contracting region. Therefore, for an increase of membrane cations' size, we predict larger (smaller) tip deflections for small (large) cations in the external solution. Accounting for hydration effects, the difference in the effective size of hydrated cations is less prominent than for bare cations, such that we expect a weak dependence of the tip displacement on the cations' size within the membrane.

Figure 2 shows the estimated range of tip displacement for a Nafion$^{\mathrm{TM}}$ actuator of length $l = 70\,\mathrm{mm}$ and semi-thickness $H = 0.1\,\mathrm{mm}$, for the four possible combinations of lithium and cesium cations in the membrane and external solution. Pile-up of cations from the external solution is the dominant mechanism of actuation, whereby the gradient is almost parallel to the direction of variation of $\Delta\bar{C}^{\mathrm{a}}_{+_{\mathrm{out}}}$. As expected, increasing the cations' size in the external solution causes a decrease in the tip displacement. The largest tip deflections are on the order of five membrane thicknesses. We attest a differential, less significant effect of membrane cations' size that depends on the sign of $\Delta\bar{C}^{\mathrm{a}}_{+_{\mathrm{in}}} - \Delta\bar{C}^{\mathrm{c}}_{+_{\mathrm{in}}}$. For small $\Delta\bar{C}^{\mathrm{a}}_{+_{\mathrm{out}}}$ and non-positive $\Delta\bar{C}^{\mathrm{a}}_{+_{\mathrm{in}}} - \Delta\bar{C}^{\mathrm{c}}_{+_{\mathrm{in}}}$, we predict zero tip deflection, whereby cathode and anode are contracting equally. Further reducing the value of either concentration change leads to negative tip deflections, against the electric field direction, since the anode is contracting more than the cathode.

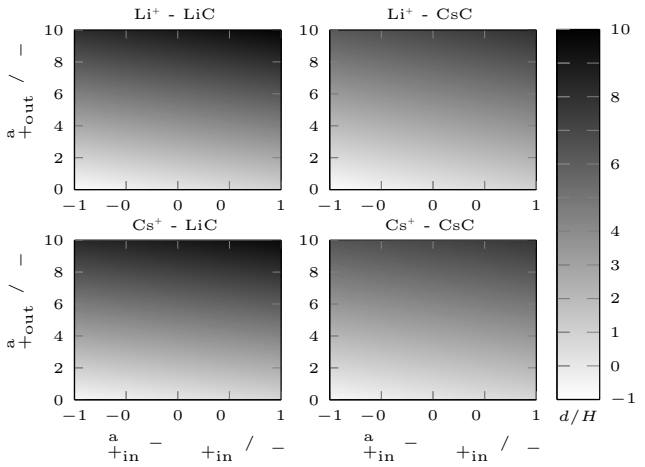

FIG. 2. Estimates of nondimensional tip displacement from Eq. (3), for different combinations of cations in the membrane and external solution. Displacements and cations' concentrations are nondimensionalized with respect to H and C_-, respectively. Positive tip displacements are in the direction of the electric field. The red dashed line indicates zero tip displacement. Average parameters in Eq. (3) are estimated as $\mathcal{V}_0 = 1.8 \times 10^{-5}\,\mathrm{m^3/mol}$, $\mathcal{V}_+ = 4.5 \times 10^{-5}\,\mathrm{m^3/mol}$, and $\lambda = 5.72 \times 10^{-10}\,\mathrm{m}$ for Nafion$^{\mathrm{TM}}$ membranes (see Supplemental Material [50–58]).

Experiments.–To verify the possibility of solvation-driven actuation and corroborate the predictions of our model, we experimentally study the response of ionic membranes in four different counterions' forms (Li^+, Na^+, K^+, and Cs^+), in four 0.1 M electrolyte solutions (LiCl, NaCl, KCl, and CsCl). Six membranes are tested for each of the 16 combinations.

The experimental setup consists of a transparent box filled with one liter of salt solution. A frame, immersed in the solution, holds two graphite electrodes at a distance $d_{\mathrm{el}} = 12\,\mathrm{mm}$. A Nafion$^{\mathrm{TM}}$-117 ionic membrane (semi-thickness $H \approx 0.1\,\mathrm{mm}$, free-length $l = 70\,\mathrm{mm}$, and width $b = 5\,\mathrm{mm}$), which previously underwent ion exchange in a 1 M solution for at least 48 hours, is mounted in a clamp and slid between the two electrodes. A laser displacement sensor measures the deflection of the membrane tip. A circuit applies across the electrodes ten voltage steps of 1 V amplitude and 60 s duration, with alternating polarity, separated by 60 s in which electrodes are shorted.

Figure 3 shows typical time traces of the tip displacement of the membranes for varying cations' type in both the external solution and membrane. For almost all conditions, we observe a consistent bending in the direction of the electric field, similar to previous experiments [21, 22]. However, when both the external solution and membrane contain large cations, membranes bend in the opposite direction. We attribute this behavior to the marginal role of solvation for large cations, with other

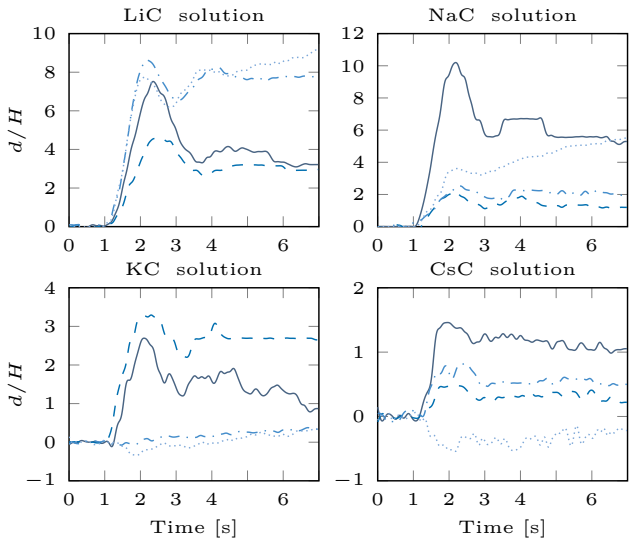

FIG. 3. Typical time traces of the tip displacement of membranes in different external solutions, following the application of a step voltage of 1 V across the external electrodes at 1 s. Solid, dashed, dotted, and dash-dotted lines indicate the response of membranes in Li^+, Na^+, K^+, and Cs^+ form, respectively. Positive tip displacements are in the direction of the electric field. Displacements are nondimensionalized with respect to H.

phenomena dominating the membrane response [24, 37].

The time profile of the tip displacement varies with the cations in the membrane. While membranes with small cations display an initial large overshoot with a progressive decrease toward a constant, lower value, large membrane cations show an initial peak followed by damped oscillations around a steady-state displacement approximately equal to the first peak, see Supplemental Material for a dynamic model [59, 60]. For each voltage step, we quantify the peak displacement of the membrane from the maximum absolute value of tip displacement in the first two seconds after the current reaches its peak. The dataset is pre-processed to remove faulty membranes and outliers.

We estimate theoretical values of peak displacement by fitting the medians of experimental peak displacements, utilizing Eq. (3) with varying h_{in} and h_{out}. We obtain the values of $\Delta\bar{C}^{\text{a}}_{+_{\text{in}}} - \Delta\bar{C}^{\text{c}}_{+_{\text{in}}}$ and $\Delta\bar{C}^{\text{a}}_{+_{\text{out}}}$ that generate the experimental peak displacements, assuming changes in cations' average concentrations are independent of cations' sizes in both the external solution and membrane. This hypothesis is justified by the averaging process over the double layers, which smears profiles' variations due to cations' sizes (see Supplemental Material [61]). To account for other forces that do not depend on solvation, such as osmotic pressure and Maxwell stress [37], we leave the constant term of Eq. (3) free and focus on trends underlying the dataset. We obtain a large adjusted R^2 value of 0.68, with estimates $\Delta\bar{C}^{\text{a}}_{+_{\text{in}}} - \Delta\bar{C}^{\text{c}}_{+_{\text{in}}} \approx 4.14 \times 10^3\,\text{mol/m}^3$ and $\Delta\bar{C}^{\text{a}}_{+_{\text{out}}} \approx 4.17 \times 10^4\,\text{mol/m}^3$ in line with our estimates on concentration changes.

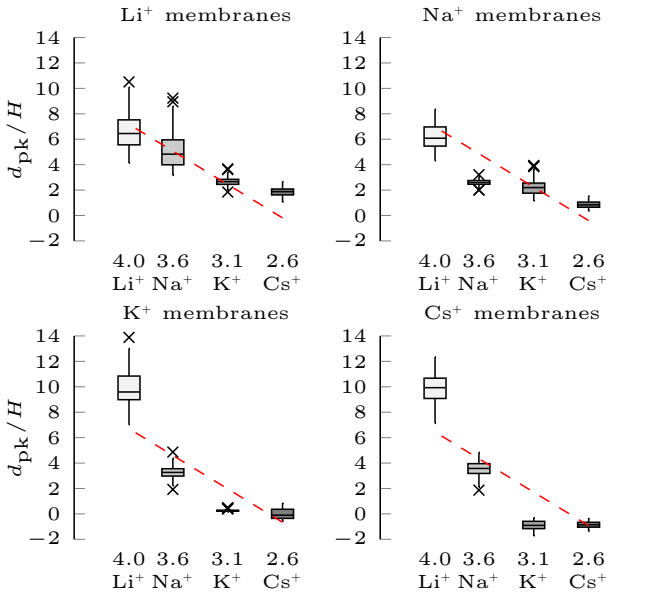

FIG. 4. Boxplot of peak displacements of membranes in different counterions' form in LiCl, NaCl, KCl, and CsCl external solutions as a function of the hydration number of cations in the external solution, and theoretical predictions (dashed red line). The thick line in the box indicates the median, the box limits identify the first and third quartiles, the whiskers delimit the 1.5-interquartile range, and crosses indicate outliers. Displacements are nondimensionalized with respect to H.

In Fig. 4, we display boxplots of peak displacement of membranes for each combination of cations in the external solution and membrane, alongside the theoretical trend. Our model can reconstruct the role of cations in the external solution, as indicated by the large R^2 value. However, our model cannot correctly predict the effect of cations in the membrane, due to the hypothesis that $\Delta\bar{C}^{\text{a}}_{+_{\text{in}}} - \Delta\bar{C}^{\text{c}}_{+_{\text{in}}}$ is independent of cations' size. In the Supplemental Material, we show that this is only due to the elementary fitting approach summarized herein.

We test our hypotheses by fitting a generalized linear mixed-effects model with Gamma family link functions [38], with cations' forms in both the external solution and membrane as explanatory variables, along with their interaction, and membrane number as random effect. We use two-way analysis of variance (ANOVA) and Tukeys honest significant difference (HSD) as a post-hoc test [38], at a significance level of 0.05.

As expected, we record a significant effect of the cations' type in both the external solution and membrane, along with their interaction ($p < 0.001$ for all). For almost all combinations, post-hoc analyses show a decrease in peak displacement for larger ions in the external solution, for the same cations in the membrane

($p < 0.001$), as predicted by our theory [39]. Post-hoc tests corroborate our hypotheses, whereby increasing the cations' size in the membrane causes an increment in peak displacement for LiCl and NaCl external solutions ($p < 0.011$) [40] and a decrease for KCl and CsCl external solutions ($p < 0.001$) [41]. In agreement with predictions from our model, the dependence of cations in the external solution is stronger than that of cations in the membrane. Supplemental Material contains experimental details and statistical analysis [62–68].

Our results challenge previous explanations of contactless actuation of ionic membranes in salt solution. Steady-state displacement with no current flow (Fig. 3) defies the theory that cations from the external solution pass through and drag the membrane in the direction of the electric field [21]. Other potential explanations entail osmotic pressure [42] and Maxwell stress [37], but these phenomena are likely to play a secondary role, see Supplemental Material [69].

Conclusions.–Here, we offered theoretically-backed, empirical evidence of the role of solvation in the mechanical response of macroscopic systems. From first principles, we established a simplified model that explains solvation-driven actuation, across a range of experimental conditions. Future research should seek to refine the theoretical model, by including a continuum description of solvation [43]. Simulations of this extended model with realistic parameters will require non-trivial numerical treatments, due to the variety of scales that must be resolved. Other microscopic phenomena modulated by the strength of cation-membrane interactions [44] could also contribute to the mechanical response of the membrane, as detailed in the Supplemental Material [70–72]. A quantitative understanding of these phenomena could be achieved through atomistic-level simulations [45].

Our work calls for an assessment of the effects of solvation on selectively-permeable membranes, widely used in fuel cells and electrolyzers [23]. Deformations caused by solvation could cause fatigue in repeated voltage applications, potentially reducing membrane operational life [46]. Solvation could also affect natural selectively-permeable membranes, including cell membranes. Given their small thickness, on the order of 10 nm, solvation may significantly affect their mechanics even with cell potentials of only 70 mV. This phenomenon has potential repercussions on cell physiology, including cell volume regulation [47], which warrant additional efforts to extend Goldman-Hodgkin-Katz equations [48] to solvation effects.

The authors acknowledge financial support from the National Science Foundation under grant No. OISE-1545857 and National Research Foundation of Korea (NRF) funded by the Korea government (MSIT) under grant No. 2020R1A2C2005252. The authors are grateful to Roni Barak Ventura and Agnieszka Truszkowska for their help with experiments and useful discussion.

* mporfiri@nyu.edu

[1] J. M. Barthel, H. Krienke, and W. Kunz, *Physical chemistry of electrolyte solutions: Modern aspects*, Vol. 5 (Springer Science & Business Media, 1998).
[2] Y. Marcus, *Ions in solution and their solvation* (John Wiley & Sons, 2015).
[3] G. N. Lewis and M. Randall, *Thermodynamics and the free energy of chemical substances* (McGraw-Hill, 1923).
[4] J. Kielland, Individual activity coefficients of ions in aqueous solutions, Journal of the American Chemical Society **59**, 1675 (1937).
[5] M. Born, Volumen und hydratationswärme der ionen, Zeitschrift für Physik **1**, 45 (1920).
[6] B. Mennucci and R. Cammi, *Continuum solvation models in chemical physics: From theory to applications* (John Wiley & Sons, 2008).
[7] L. X. Dang, J. E. Rice, J. Caldwell, and P. A. Kollman, Ion solvation in polarizable water: Molecular dynamics simulations, Journal of the American Chemical Society **113**, 2481 (1991).
[8] J. Tomasi, B. Mennucci, and R. Cammi, Quantum mechanical continuum solvation models, Chemical Reviews **105**, 2999 (2005).
[9] W. Jarzeba, G. C. Walker, A. E. Johnson, M. A. Kahlow, and P. F. Barbara, Femtosecond microscopic solvation dynamics of aqueous solutions, The Journal of Physical Chemistry **92**, 7039 (1988).
[10] R. Jimenez, G. R. Fleming, P. Kumar, and M. Maroncelli, Femtosecond solvation dynamics of water, Nature **369**, 471 (1994).
[11] Y. Marcus, Effect of ions on the structure of water: Structure making and breaking, Chemical Reviews **109**, 1346 (2009).
[12] Y. Marcus, *Ions in water and biophysical implications: From chaos to cosmos* (Springer Science & Business Media, 2012).
[13] M. Andreev, J. J. de Pablo, A. Chremos, and J. F. Douglas, Influence of ion solvation on the properties of electrolyte solutions, The Journal of Physical Chemistry B **122**, 4029 (2018).
[14] M. Hey, J. Clough, and D. Taylor, Ion effects on macromolecules in aqueous solution, Nature **262**, 807 (1976).
[15] P. Jungwirth and D. J. Tobias, Specific ion effects at the air/water interface, Chemical Reviews **106**, 1259 (2006).
[16] C. Reichardt and T. Welton, *Solvents and solvent effects in organic chemistry* (John Wiley & Sons, 2011).
[17] H. Hansen-Goos, R. Roth, K. Mecke, and S. Dietrich, Solvation of proteins: Linking thermodynamics to geometry, Physical Review Letters **99**, 128101 (2007).
[18] A. Salis and B. W. Ninham, Models and mechanisms of Hofmeister effects in electrolyte solutions, and colloid and protein systems revisited, Chemical Society Reviews **43**, 7358 (2014).
[19] T. Shiga and T. Kurauchi, Deformation of polyelectrolyte gels under the influence of electric field, Journal of Applied Polymer Science **39**, 2305 (1990).
[20] P. Grimshaw, A. Grodzinsky, M. Yarmush, and D. Yarmush, Selective augmentation of macromolecular transport in gels by electrodiffusion and electrokinetics, Chemical Engineering Science **45**, 2917 (1990).
[21] K. J. Kim, V. Palmre, T. Stalbaum, T. Hwang, Q. Shen,

and S. Trabia, Promising developments in marine applications with artificial muscles: Electrodeless artificial cilia microfibers, Marine Technology Society **50**, 24 (2016).

[22] A. Boldini, M. Rosen, Y. Cha, and M. Porfiri, Contactless actuation of perfluorinated ionomer membranes in salt solution: An experimental investigation, Scientific Reports **9**, 1 (2019).

[23] Y. Tanaka, *Ion exchange membranes – Fundamentals and applications*, 2nd ed. (Elsevier, 2015).

[24] A. Boldini, M. Rosen, Y. Cha, and M. Porfiri, Modeling actuation of ionomer cilia in salt solution under an external electric field, ASME Letters in Dynamic Systems and Control **1**.

[25] M. J. Cheah, I. G. Kevrekidis, and J. Benziger, Effect of interfacial water transport resistance on coupled proton and water transport across Nafion, The Journal of Physical Chemistry B **115**, 10239 (2011).

[26] Molecular dynamics simulations have shown that there are significant effects on solvation shells only for large external electric fields [49].

[27] W. Hong, X. Zhao, and Z. Suo, Large deformation and electrochemistry of polyelectrolyte gels, Journal of the Mechanics and Physics of Solids **58**, 558 (2010).

[28] J. Y. Li and S. Nemat-Nasser, Micromechanical analysis of ionic clustering in Nafion perfluorinated membrane, Mechanics of Materials **32**, 303 (2000).

[29] I. Benjamin, Structure and dynamics of hydrated ions in a water-immiscible organic solvent, The Journal of Physical Chemistry B **112**, 15801 (2008).

[30] D. Rose and I. Benjamin, Free energy of transfer of hydrated ion clusters from water to an immiscible organic solvent, The Journal of Physical Chemistry B **113**, 9296 (2009).

[31] Estimating average hydration numbers from macroscopic thermodynamics quantities of the solution provides analogous results, see Supplementary Material.

[32] A. J. Bard and L. R. Faulkner, *Electrochemical methods - Fundamentals and applications* (John Wiley & Sons, 2001).

[33] M. S. Kilic, M. Z. Bazant, and A. Ajdari, Steric effects in the dynamics of electrolytes at large applied voltages. I. Double-layer charging, Physical Review E **75** (2007).

[34] In the Supplemental Material, we show a parametric analysis for different values of ζ.

[35] S. Nemat-Nasser and J. Y. Li, Electromechanical response of ionic polymer-metal composites, Journal of Applied Physics **87** (2000).

[36] M. Porfiri, Influence of electrode surface roughness and steric effects on the nonlinear electromechanical behavior of ionic polymer metal composites, Physical Review E **79** (2009).

[37] Y. Cha and M. Porfiri, Mechanics and electrochemistry of ionic polymer metal composites, Journal of the Mechanics and Physics of Solids **71**, 156 (2014).

[38] C. M. Judd, G. H. McClelland, and C. S. Ryan, *Data analysis: A model comparison approach to regression, ANOVA, and beyond*, 3rd ed. (Taylor&Francis, 2017).

[39] Three pairwise comparisons, $Na^+ - NaCl$ against $Na^+ - KCl$, $K^+ - KCl$ against $K^+ - CsCl$, and $Cs^+ - KCl$ against $Cs^+ - CsCl$, are not significant ($p > 0.754$).

[40] Three comparisons are not significantly different ($p > 0.382$): $Li^+ - LiCl$ against $Na^+ - LiCl$, $K^+ - LiCl$ against $Cs^+ - LiCl$, and $K^+ - NaCl$ against $Cs^+ - NaCl$. Comparisons $Li^+ - NaCl$ against $Na^+ - NaCl$, $Li^+ - NaCl$ against $K^+ - NaCl$, and $Li^+ - NaCl$ against $Cs^+ - NaCl$ indicate a significant decrease in peak displacement for larger membrane cations ($p < 0.001$).

[41] The only non-significant comparison is $Li^+ - KCl$ against $Na^+ - KCl$ ($p = 0.505$).

[42] This term indirectly includes the effect of the migration of water molecules to re-establish constant (electro)chemical potentials throughout the system [37].

[43] A. R. Crothers, R. M. Darling, A. Kusoglu, C. J. Radke, and A. Z. Weber, Theory of multicomponent phenomena in cation-exchange membranes: Part I. Thermodynamic model and validation, Journal of The Electrochemical Society **167**, 013547 (2020).

[44] S. Shi, A. Z. Weber, and A. Kusoglu, Structure-transport relationship of perfluorosulfonic-acid membranes in different cationic forms, Electrochimica Acta **220**, 517 (2016).

[45] A. Venkatnathan, R. Devanathan, and M. Dupuis, Atomistic simulations of hydrated Nafion and temperature effects on hydronium ion mobility, The Journal of Physical Chemistry B **111**, 7234 (2007).

[46] M. Pestrak, Y. Li, S. W. Case, D. A. Dillard, M. W. Ellis, Y.-H. Lai, and C. S. Gittleman, The effect of mechanical fatigue on the lifetimes of membrane electrode assemblies, Journal of Fuel Cell Science and Technology **7** (2010).

[47] E. K. Hoffmann, I. H. Lambert, and S. F. Pedersen, Physiology of cell volume regulation in vertebrates, Physiological Reviews **89**, 193 (2009).

[48] G. A. Truskey, F. Yuan, and D. F. Katz, *Transport phenomena in biological systems* (Pearson/Prentice Hall, 2004).

[49] Z. He, H. Cui, S. Hao, L. Wang, and J. Zhou, Electric-field effects on ionic hydration: A molecular dynamics study, The Journal of Physical Chemistry B **122**, 5991 (2018).

[50] R. Jia, B. Han, K. Levi, T. Hasegawa, J. Ye, and R. H. Dauskardt, Effect of cation contamination and hydrated pressure loading on the mechanical properties of proton exchange membranes, Journal of Power Sources **196**, 3803 (2011).

[51] M. Bass and V. Freger, Hydration of Nafion and Dowex in liquid and vapor environment: Schroeder's paradox and microstructure, Polymer **49**, 497 (2008).

[52] S. Sengupta and A. V. Lyulin, Molecular dynamics simulations of substrate hydrophilicity and confinement effects in capped Nafion films, The Journal of Physical Chemistry B **122**, 6107 (2018).

[53] A. Stracuzzi, E. Mazza, and A. E. Ehret, Chemomechanical models for soft tissues based on the reconciliation of porous media and swelling polymer theories, ZAMM-Journal of Applied Mathematics and Mechanics/Zeitschrift für Angewandte Mathematik und Mechanik **98**, 2135 (2018).

[54] M. E. Gurtin, E. Fried, and L. Anand, *The Mechanics and Thermodynamics of Continua* (Cambridge University Press, 2013).

[55] S. Nemat-Nasser and Y. Wu, Comparative experimental study of ionic polymer–metal composites with different backbone ionomers and in various cation forms, Journal of Applied Physics **93**, 5255 (2003).

[56] M. Porfiri, An electromechanical model for sensing and actuation of ionic polymer metal composites, Smart Ma-

terials and Structures **18** (2009).

[57] T. D. Gierke, G. E. Munn, and F. C. Wilson, The morphology in Nafion perfluorinated membrane products, as determined by wide- and small-angle x-ray studies, Journal of Polymer Science: Polymer Physics Edition **19**, 1687 (1981).

[58] Y. Cha, M. Aureli, and M. Porfiri, A physics-based model of the electrical impedance of ionic polymer metal composites, Journal of Applied Physics **111**, (2012).

[59] L. Meirovitch, *Fundamentals of Vibrations*, international ed. (McGraw Hill, 2001).

[60] M. Aureli, M. E. Basaran, and M. Porfiri, Nonlinear finite amplitude vibrations of sharp-edged beams in viscous fluids, Journal of Sound and Vibration **331**, 1624 (2012).

[61] M. S. Kilic, M. Z. Bazant, and A. Ajdari, Steric effects in the dynamics of electrolytes at large applied voltages. II. Modified Poisson-Nernst-Planck equations, Physical Review E **75** (2007).

[62] N. An, B. Zhuang, M. Li, Y. Lu, and Z.-G. Wang, Combined theoretical and experimental study of refractive indices of water–acetonitrile–salt systems, The Journal of Physical Chemistry B **119**, 10701 (2015).

[63] K. P. Burnham and D. R. Anderson, Multimodel inference – Understanding AIC and BIC in model selection, Sociological Methods & Research **33**, 261 (2004).

[64] R Core Team, *R: A Language and Environment for Statistical Computing*, R Foundation for Statistical Computing (2013).

[65] D. Bates, M. Mächler, B. Bolker, and S. Walker, Fitting linear mixed-effects models using lme4, Journal of Statistical Software **67**, 1 (2015).

[66] K. Barton, *MuMIn: Multi-Model Inference,* (2019), R package version 1.43.6.

[67] J. Fox and S. Weisberg, *An R Companion to Applied Regression*, 2nd ed. (Sage, 2011).

[68] R. Lenth, *emmeans: Estimated Marginal Means, aka Least-Squares Means* (2019), r package version 1.3.4.

[69] A. Boldini, M. Rosen, Y. Cha, and M. Porfiri, Searching for clues about Maxwell stress in the back-relaxation of ionic polymer-metal composites, in *Proceedings of SPIE 10966*, Vol. Electroactive Polymer Actuators and Devices (EAPAD) XXI, 109661K (2019).

[70] S. C. Yeo and A. Eisenberg, Physical properties and supermolecular structure of perfluorinated ion-containing (Nafion) polymers, Journal of Applied Polymer Science **21**, 875 (1977).

[71] M. Fujimura, T. Hashimoto, and H. Kawai, Small-angle X-ray scattering study of perfluorinated ionomer membranes. 1. Origin of two scattering maxima, Macromolecules **14**, 1309 (1981).

[72] R. Hammer, M. Schöïhoff, and M. R. Hansen, Comprehensive picture of water dynamics in Nafion membranes at different levels of hydration, The Journal of Physical Chemistry B **123**, 8313 (2019).